A STRUCTURAL ANALYSIS OF THE MYELIN SHEATH IN THE CENTRAL NERVOUS SYSTEM

ASAO HIRANO and HERBERT M. DEMBITZER

From the Henry and Lucy Moses Research Laboratories of the Laboratory Division, Montefiore Hospital and Medical Center, Bronx, New York 10467

ABSTRACT

The cerebral white matter of rats subjected to a variety of noxious experimental conditions was examined in the electron microscope. Several unusual configurations of the myelin sheath are identified in addition to the usual configuration. These variations include the presence of (*a*) formed organelles within the inner and outer loops, (*b*) isolated islands of cytoplasm in unfused portions of the major dense lines, (*c*) apparently unconnected cell processes between the sheath and the axon, and (*d*) concentric, double myelin sheaths. A generalized model of the myelin sheath based on a hypothetical unrolling of the sheath is described. It consists of a shovel-shaped myelin sheet surrounded by a continuous thickened rim of cytoplasm. Most of the unusual myelin configurations are explained as simple variations on this basic theme. With the help of this model, an explanation of the formation of the myelin sheath is offered. This explanation involves the concept that myelin formation can occur at all cytoplasmic areas adjacent to the myelin proper and that adjacent myelin lamellae can move in relation to each other.

By now, the theory of spiral wrapping by a single cell process is generally accepted as the main method by which myelin is formed in the vertebrate central nervous system, both in myelinogenesis and in remyelination (5–7, 11, 18, 25, 26, 28, 29–31, 34, 36, 37). The great majority of published micrographs and, indeed, those seen in our own laboratory may be interpreted on this basis. Occasionally, however, profiles of the myelin sheath are observed which, while they do not speak against the spiral-wrapping theory, require a more complex explanation than the simple uniform wrapping of a myelin-forming cell process around an axon.

These profiles, relatively rare under normal conditions, are quite frequent under pathological or experimental conditions. Such profiles include those showing isolated cytoplasmic islands within incompletely fused major dense lines (6, 11, 26), unconnected cell processes between the innermost myelin lamallae and the axons (6, 19, 29, 34), and double, concentric sheaths surrounding a single axon (11, 13).

It is the purpose of the present paper to describe these configurations under a variety of experimental conditions and to present a uniform, generalized model of the myelin sheath in the central nervous system basically similar to that presented by Robertson (33) for the peripheral nervous system. This model not only will, we feel, serve to explain the anatomy of most of the above mentioned configurations but, also will be useful in explaining some of the processes involved in myelinogenesis and remyelination.

MATERIALS AND METHODS

Several experimental procedures were used in the present study, all of which yielded essentially similar results. The procedures included cyanide intoxication (9, 22), experimental allergic encephalomyelitis (17), dibenzanthracene implantation (3, 12), cold injury (14, 20, 35), and *Cryptococcus neoformans* (21) as well as purified cryptococcal polysaccharide im-

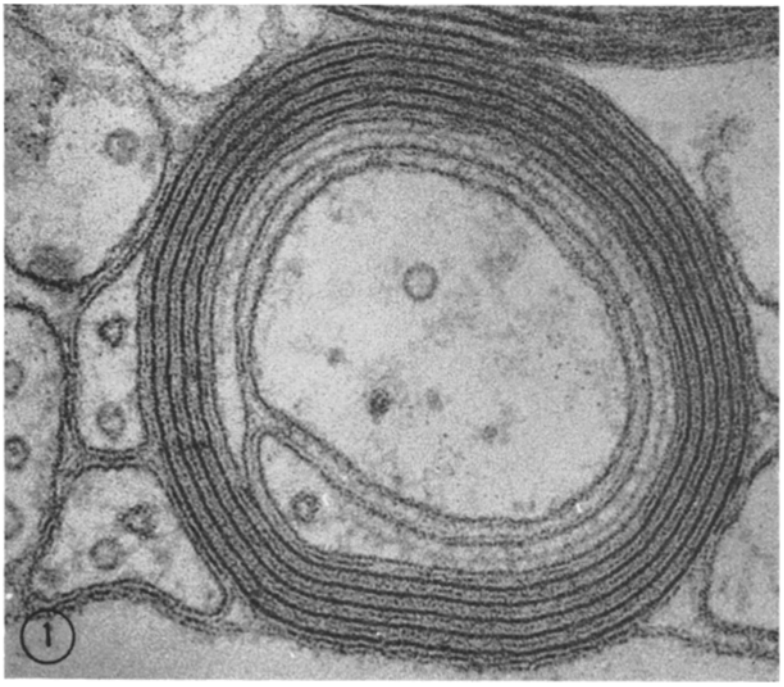

FIGURE 1 A type A myelinated axon in nonedematous white matter from a rat subjected to cyanide intoxication. × 166,000.

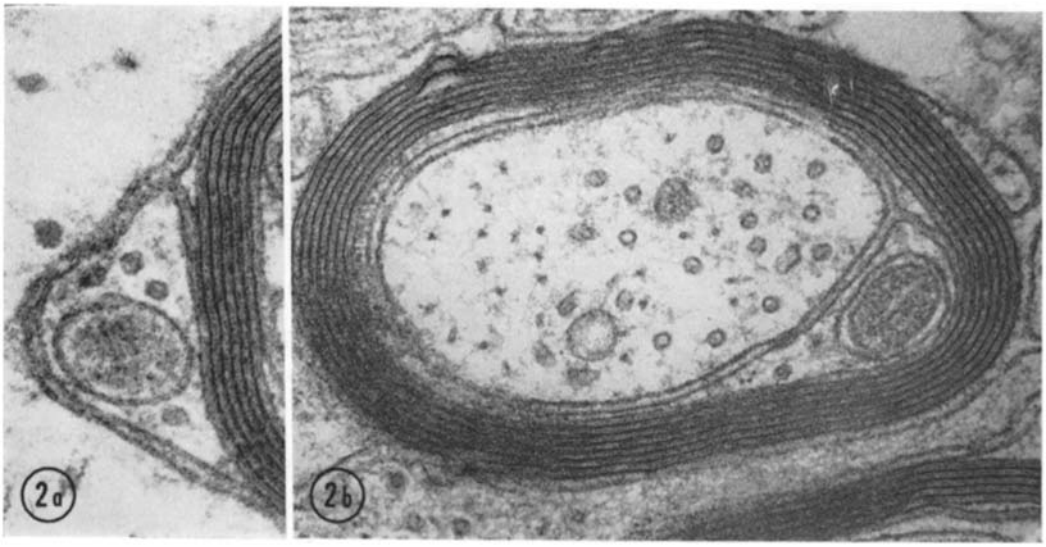

FIGURE 2 *a*, A portion of a type B myelin sheath from a dibenzanthracene-implanted brain. A dense body and four microtubules are visible in the outer loop. *b*, A type B myelin sheath from the same animal as in Fig. 2 *a*. A mitochondrion and a microtubule are evident in the inner loop. *a*, × 100,000; *b*, × 90,000.

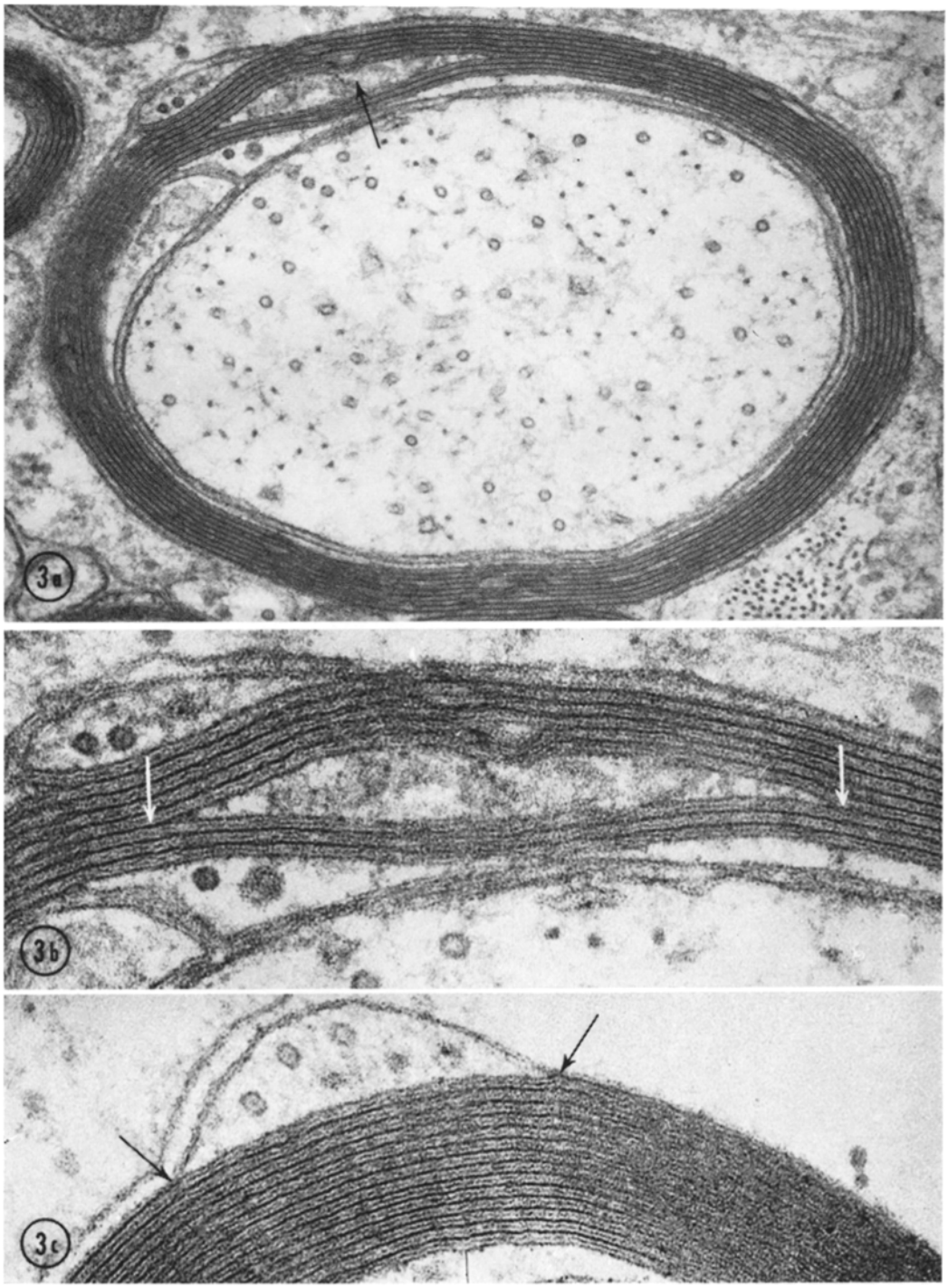

FIGURE 3 *a*, A type C myelin sheath from a dibenzanthracene-implanted brain. In addition to the inner and outer loops, an isolated cytoplasmic island is visible at the arrow. *b* Higher magnification of the cytoplasmic island visible in Fig. 3 *a*. The cytoplasmic island arises within an unfused portion of a major dense line as may be seen at the arrows. *c*, A portion of a type C myelin sheath from the brain of a cyanide-treated animal. An isolated cytoplasmic island may be seen within an unfused portion of the outermost major dense line at the arrows. Several microtubules are visible within the cytoplasmic island. *a*, × 60,000; *b*, × 135,000; *c*, × 144,000.

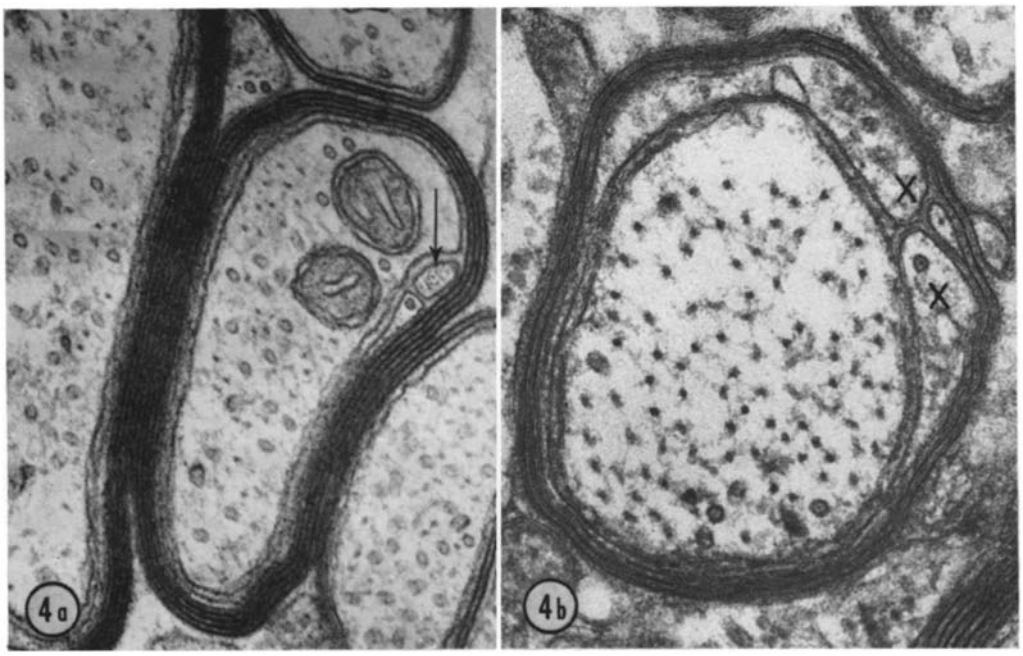

FIGURE 4 *a*, A type D myelin sheath from a dibenzanthracene-implanted brain. An apparently unconnected cell process is visible (arrow) between the innermost lamella and the axon adjacent to the inner loop. *b*, A type D myelin sheath from the brain of a cyanide-treated rat. An apparently unconnected cell process (*X*) envelopes the axon under the innermost lamella of the sheath. *a*, × 64,000; *b*, × 90,000.

plantation (10, 23). In all of the implantation experiments, pellets were placed unilaterally in the frontal white matter. The reader is referred to the cited references for details of the procedures. The animals were sacrificed in the chronic stages, i.e., at least 1 wk after the experimental procedure.

Fixation was by intravascular perfusion (27) with 5.0% glutaraldehyde in 1/15 M phosphate buffer at pH 7.4. After perfusion with about 100 ml of perfusate, the corpus callosum and the callosal radiation were dissected out, cut into small fragments, and immersed in Dalton's fluid (8) for about 1 hr. Dehydration was accomplished in an ascending series of alcohols and embedding was done in Luft's (24) Epon. Thin sections were cut on a Porter-Blum MT-1 ultramicrotome with a diamond knife and were observed in a Siemens IA electron microscope subsequent to uranyl and lead staining.

RESULTS

We have been able to classify various configurations of the myelin sheath into five categories. It must be emphasized that each category was seen in all of the experimental conditions described above.

TYPE A: This type was the most common one seen in our experience (Fig. 1). It consisted of several myelin lamellae around the axon. The only cytoplasm visible in the myelin-forming cell was in the inner and outer loops which contained no formed organelles, except for a few microtubules and perhaps a vesicle or two. A single, continuous spiral could be traced from the outer to the inner loop.

This configuration was the usual one and, of course, was seen in normal tissue. The four other configurations decsribed below were fairly common in the experimental conditions but, while most were present in normal tissue, usually they were extremely rare.

TYPE B: In the second category of configurations, the myelin sheath was indistinguishable from the type A described above, except for the presence of formed organelles such as mitochondria and dense bodies in the inner and/or outer loops (11) (Fig. 2 *a–b*). This condition is often accompanied by relatively thick and long outer loops. However, we have not been able to observe

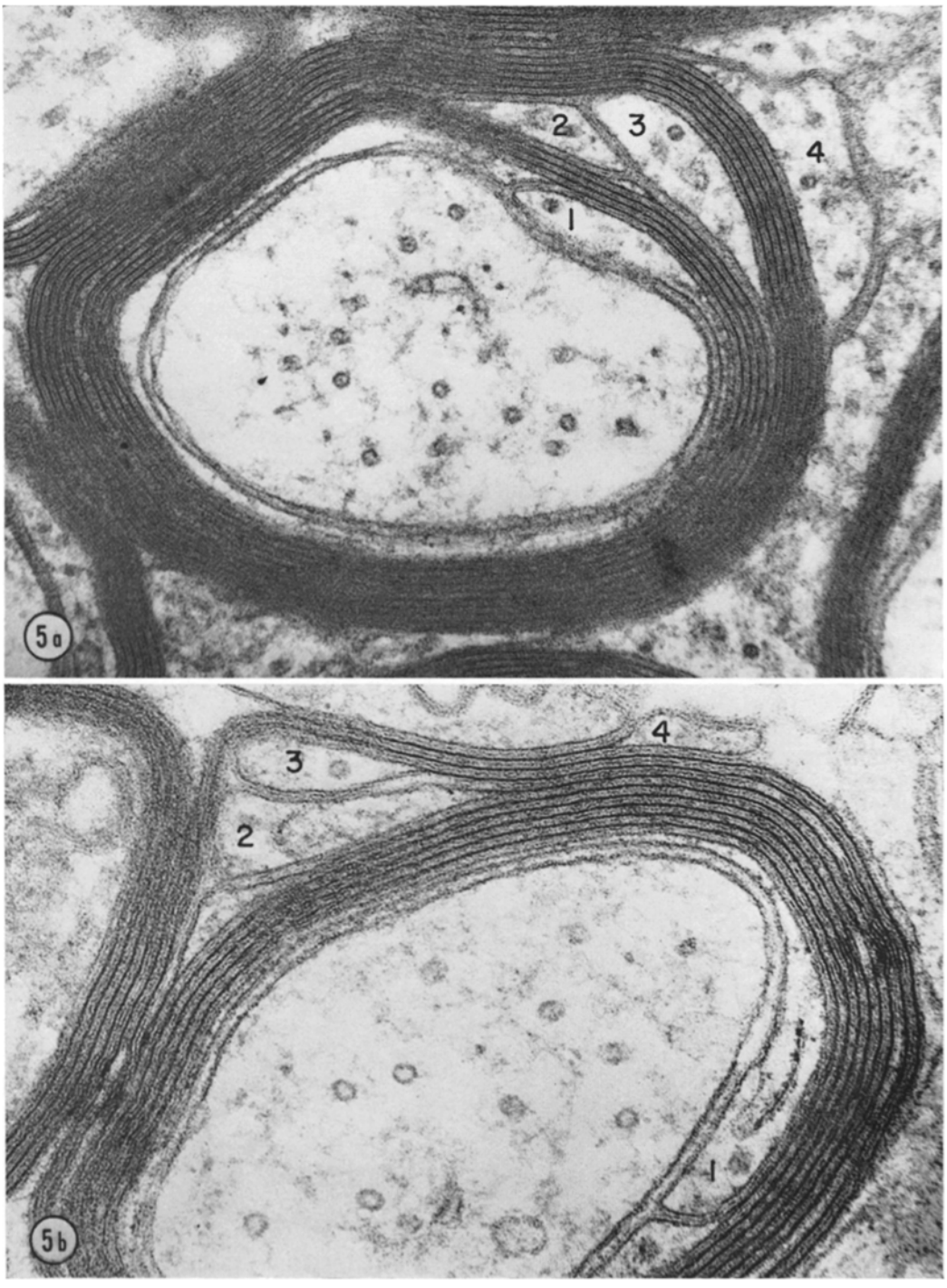

FIGURE 5 *a*, A type E myelin sheath from a dibenzanthracene implanted brain. Two distinct myelin sheaths, both spiraling in the same direction, are present. The inner (*1*) and outer (*2*) loops of the internal sheath as well as the inner (*3*) and outer (*4*) loops of the external sheath are visible. *b*, A type E myelin sheath from a dibenzanthracene implanted brain. Two distinct myelin sheaths, each spiraling in opposite directions, are present. The inner (*1*) and outer (*2*) loops of the internal sheath and the inner (*3*) and outer (*4*) loops of the external sheath are visible. *a*, × 80,000; *b*, × 112,000.

a connection between the outer loop and the myelin-forming cell perikaryon.

TYPE C: In the two categories described above, the visible cytoplasm of the myelin sheath, as seen in cross-section, was limited to the inner and outer loops. In the type C configuration, however, occasional islands of cytoplasm (6, 11, 26) were seen among the myelin lamellae themselves (Fig. 3 *a–c*). It was clear that these islands represented unfused portions of the major dense lines.

TYPE D: In the fourth category of myelin sheath configurations a cell process, apparently unconnected to either the myelin sheath or the axon (6, 34), was visible between the innermost myelin lamella and the axon (Fig. 4 *a–b*). Up to eight such unconnected processes have been counted in a single cross-section of a myelin sheath. Occasionally, a single unconnected process was apparently sheetlike and surrounded the axon at least partially (Fig. 4 *b*).

TYPE E: The last category of myelin sheath configurations that we shall describe was somewhat similar to the type D configuration in that two cell processes were present in addition to the axon. In the type E configuration, however, both processes had formed several myelin lamellae and thus resulted in two concentric myelin sheaths around a single axon (Fig. 5 *a–b*). Each sheath was equipped with its own inner and outer loops (11, 13). The sheaths spiralled in the same (Fig. 5 *a*) or in opposite (Fig. 5 *b*) directions and had roughly equal or quite unequal numbers of turns.

Because of our experimental conditions, internodal distances were relatively short, and longitudinal sections through the nodes of Ranvier were frequently observed. At the nodes, several or many lateral loops were present. In most instances each was connected to a single myelin lamella (Fig. 6 *a*). On a few occasions, however, the loops were continuous with long cytoplasmic processes penetrating between the myelin lamellae arising from adjacent loops. Most often, the long cytoplasmic processes seen in longitudinal sections arose from the innermost and outermost lateral loops. Occasionally, some of the lateral loops contained a formed organelle such as a mitochondrion or a dense body in addition to the usual microtubules, vesicles, and electron-opaque granules (Fig. 6 *a*).

Between the lateral loops and the axon, the external leaflet of the axolemma was differentiated into a series of regularly spaced densities approximately 100–150 A in diameter (Fig. 6 *a–b*). In transverse sections through the nodes they were sometimes visible as dense material between the lateral loop and the internal leaflet of the axolemma (Fig. 7).

DISCUSSION

On the basis of our observations of both the usual and unusual myelin sheath configurations, we have constructed a relatively simple, generalized model of the myelin sheath that, we feel, will serve to explain the variety of profiles seen in the electron microscope. Up to now, the most acceptable model of central myelin was presented by Bunge et al. (6); from this model we derived, with some modifications, our Fig. 8 *a–b*.

If one were to unroll the myelin sheath (Fig. 8 *c*), the resulting structure would be a shovel-shaped myelin sheet surrounded by a thicker, continuous rim of cytoplasm similar to that illustrated in Fig. 8 *d*. In cross-section, the "outer" and "inner" cytoplasmic rims are represented, of course, by the outer and inner loops, respectively. The lateral edges are derived from the unrolled lateral loops which are seen in longitudinal sections through the nodes of Ranvier.

It is to be emphasized that according to our model all the loops, i.e. the inner, outer, and lateral, are directly continuous with each other (30). Furthermore, they are also presumably continuous with the perikaryon of the myelin-forming cell, at least during myelin formation. Thus, the impression often gained from the cross-sectional view, that the inner and outer loops in mature myelin communicate only through the myelin lamellae, is false. On this basis, we may explain the often noticed (25, 26, 28) observation that the texture, density, and included organelles of all of the loops are remarkably similar under all circumstances.

Since the transverse dense bands seen between the lateral loops and the axons are, in reality, differentiations of the axonal plasma membrane, we must assume that they arise as a reaction to the contact between the lateral rims and the axon (Fig. 8 *a* and 8 *d*). They have been seen in normal tissue by several authors (2, 4, 15, 16, 32), some of whom suggested that they might be either a series of parallel groups of bands or a continuous spiral arrangement of 6–8 bands. While we cannot draw any definite conclusions, it does not seem unreasonable to assume that the bands follow the

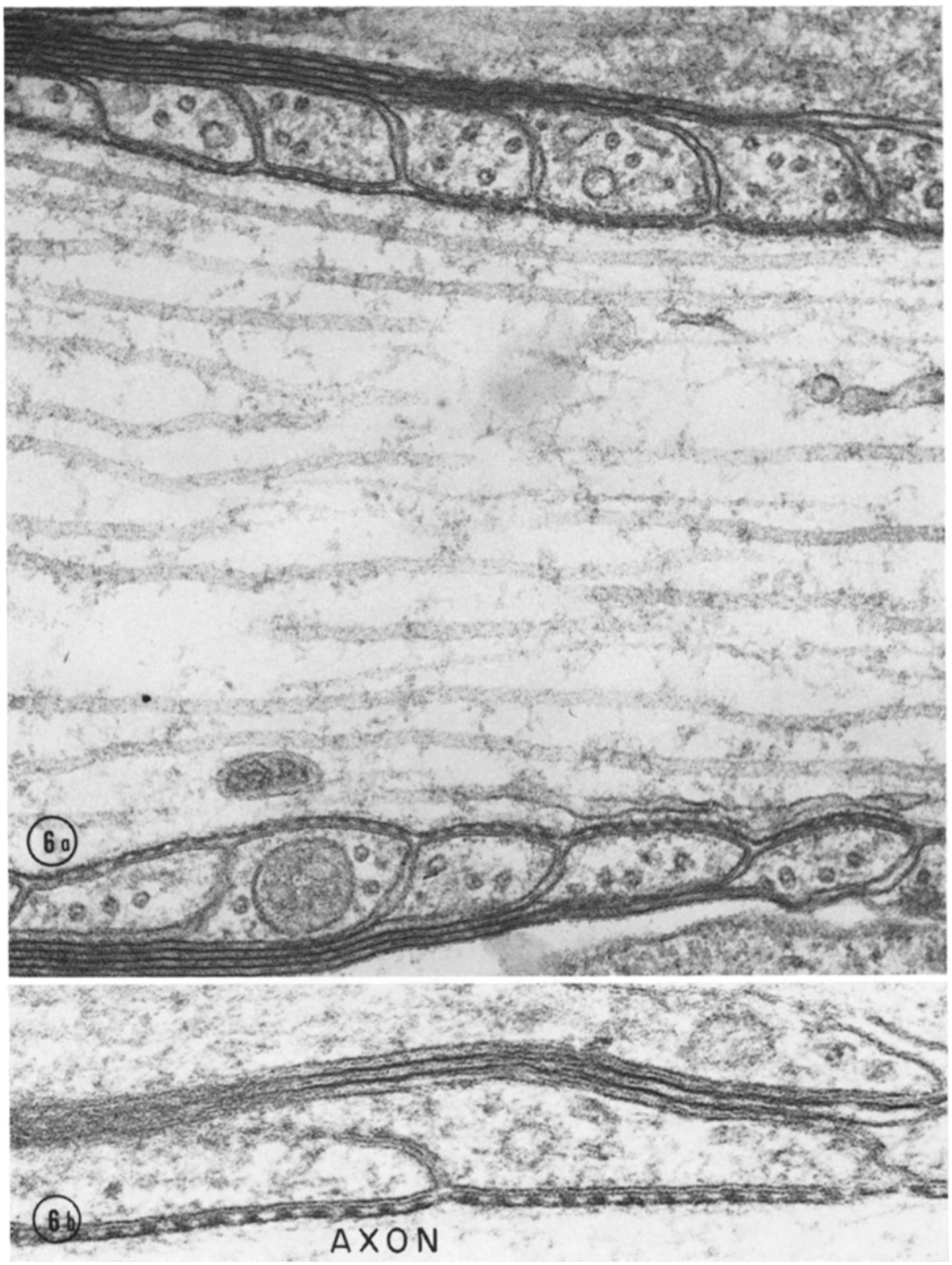

FIGURE 6 *a*, A longitudinal section of a myelinated axon near a node of Ranvier in the brain of a cyanide-treated rat. Several lateral loops, each connected to a single major dense line, are visible on both sides of the axon. A dense body is present in one lateral loop, and microtubules are present in all the loops. Evenly spaced densities are clearly visible between the lateral loops and the axon. *b* Higher magnification of a section similar to Fig. 6 *a*. Both leaflets of the unit membrane of the lateral loops are continuous and are particularly distinct at the axonal border. The external leaflet of the axonal unit membrane is disrupted to form the evenly spaced densities. *a*, × 100,000; *b*, 160,000.

FIGURE 7 Cross-section of three axons (*1*, *2*, *3*) in the brain of a cyanide-treated rat. Axon 1 is surrounded by a cell process within an electron-lucent space between the adjacent plasma membranes. Axons 2 and 3 are probably sectioned through a paranodal level. Between axon 2 and its encircling cell process, an electron opaque material is present indicating that the section passes through a density circling the axon. Between axon 3 and its encircling cell process, part of the space is also electron opaque (arrow). × 128,000.

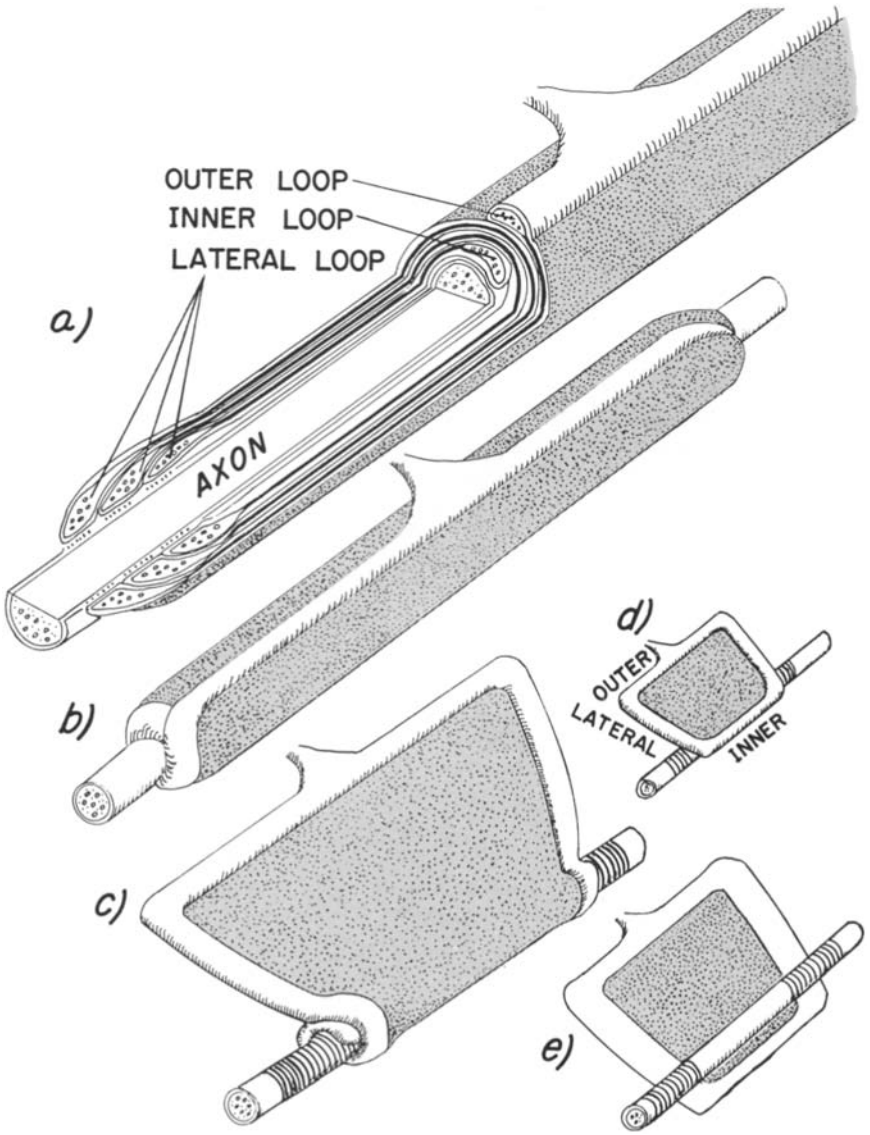

FIGURE 8 *a*, Diagram of a myelinated axon, modified after Bunge et al. (6). Part of the myelin is cut away to show the relationship between the lateral loops and the lamellae as well as between the inner loops and the axon and between the outer loop and the connection to the myelin-forming cell. Note the periodic densities, representing sections through the transverse bands between the lateral loops and the axon. *b*, Diagram of the intact myelin sheath around an axon. *c*, Diagram of the results of partially unrolling the intact sheath from around the axon. *d*, Diagram of a fully unrolled myelin sheath. The resulting shovel-shaped myelin sheet is bordered on four sides by a continuous thickened rim of cytoplasm. The outer rim, when seen in section, is represented by the outer loop, and is longer than the inner rim which is represented by the inner loop in cross-section. The lateral rims are probably of equal length and are represented by the lateral loops in longitudinal sections through the nodes of Ranvier. *e*, A diagram similar to Fig. 8 *d* but showing the surface of the sheet that contacts the axon. The transverse bands are indicated by the parallel, curved lines around the axon.

helical path of the lateral loops around the axon (Fig. 8 *e*).

All of the myelin configurations described above may be explained on the basis of minor variations of the shovel-shaped myelin sheet (Fig. 9). We feel that types A, B, and C can be explained by no other model, although the cytoplasmic area intruding into the myelin in Fig. 9 *C* may not necessarily be continuous with the lateral cytoplasmic rim. Serial cross-sections would be needed to ascertain this.

The Type D myelin configuration (Fig. 9 *D'*) may be explained by the presence of a completely separate cell process extending down the axon under the innermost myelin lamella (6, 17, 19). On the other hand, a variation in the myelin sheet such as that illustrated in Fig. 9 *D* would also account for the observed cross-sectional image.

Similarly, the type E configuration (Fig. 9 *E'*) may be explained on the basis of a variation in the myelin sheet as pictured in Fig. 9 *E*. However, when one considers the fact that, as will be explained below, the outer loop cannot rotate around the axon, at least for those cases in which the two sheaths spiral in opposite directions, one must assume the presence of a completely separate myelin-forming cell process. In that case, of course, two separate sheets, each similar to that labeled 9 *A*, would be involved.

It should be pointed out that all of these variations are observed, for the most part, during the recovery stage of a white-matter lesion. As such, they are probably not representative of the fully recovered tissue. One might, therefore, speculate that any or all of these variations, except for the type E configuration when the sheaths spiral in opposite directions, might eventually become completely normal, such as that represented in Fig. 9 *A*. Furthermore, these variations may occur in normal myelinogenesis, but more likely they are found only in a chronic lesion in the adult animal where conditions are quite different from those in the developing animal.

As shown in Fig. 9 *F* and 9 *F'*, we have extended the model to include peripheral myelin. The only difference in the myelin sheet between normal peripheral myelin (Fig. 9 *F*) and normal central myelin (Fig. 9 *A*), according to our model, is the presence of a wider cytoplasmic rim, including the nucleus, and the presence of two vertical cytoplasmic ridges, representing the Schmidt-Lantermann incisures, in the peripheral myelin. In addition, of course, a basement membrane is present at the outer cytoplasmic rim.

This model, in addition to providing us with a simple structural concept of the mature myelin sheath, perhaps, may also be useful in explaining some of the dynamic aspects of myelin sheath formation. Unless one assumes that myelin formation can occur by the addition of molecules within the sheet itself, he is left with the fact that some contiguous cytoplasmic area must be involved in myelin formation. On the basis of the continuity of the cytoplasmic rim in our model, we may reasonably consider the possibility that myelin formation occurs at the outer loop, the inner loop, the lateral loops, or any combination of these. In the following, we shall systematically examine all of these theoretical possibilities.

The possibility that myelin formation occurs only at one site may be immediately rejected.

First, if myelin formation occurred exclusively at the outer loop, there would be no increase in the internodal length of the inner lamellae, and the myelin sheet, as diagrammed in Fig. 9 *A*, would be pointed at the inner rim. This is contrary to the observed fact that the internodal lengths of the inner lamellae increase during development.

Second, we may rule out the possibility that only the inner loop produces myelin. If this were true, then either the innermost lamella would be longer than the outermost lamella, which is opposite the observed fact, or the innermost lamella would have to constantly grow narrower throughout development while the number of turns increased. The latter is, of course, impossible since the observed fact, again, is that the internodal length of the innermost lamella increases during development.

Third, a possibility to be considered is that the lateral loops alone produced myelin. We must reject this possibility too: if it were true, the internodal length of the sheath would, indeed, enlarge but the number of turns would not increase.

Thus, since no one site of myelin formation suffices to explain the observed facts, at least two types of loops must participate in the formation of the myelin sheath. We know that myelin formation must occur at the lateral loops, in order for the internodal distance of each lamella to increase, because no structures comparable to the incisures of Schmit-Lantermann are present in the central nervous system (25). The question remains: is it

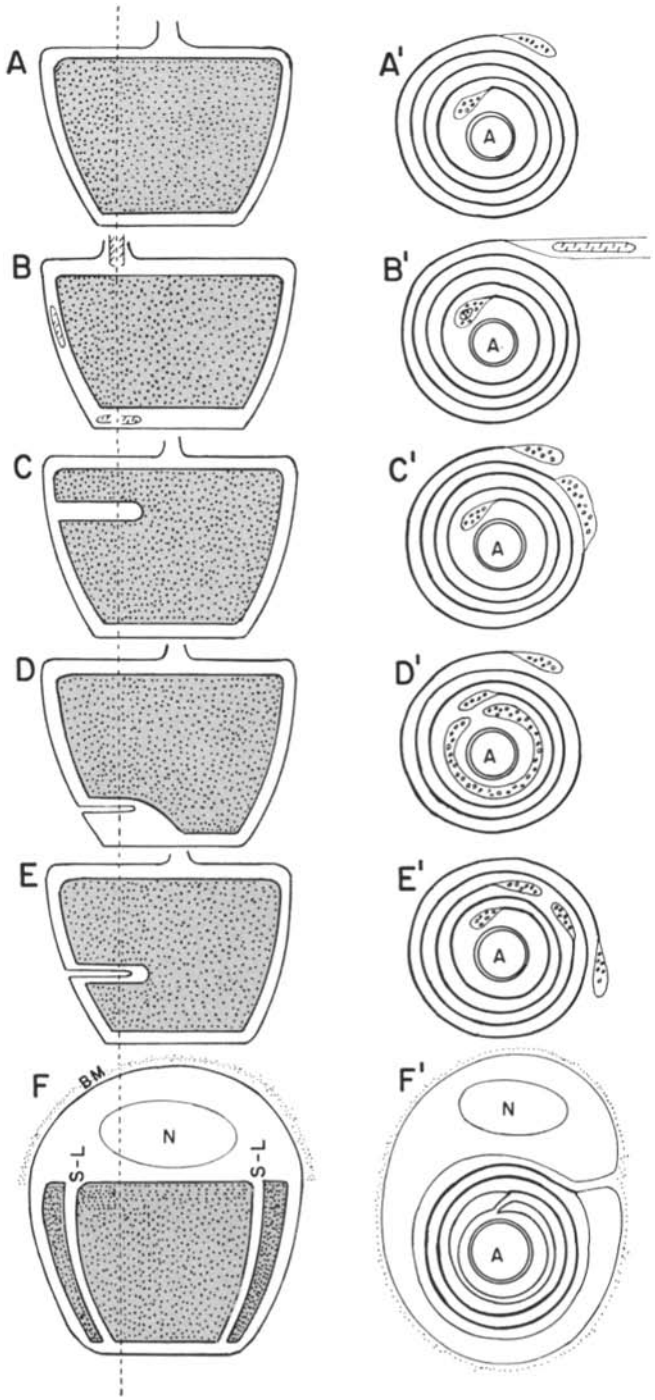

FIGURE 9 *A*, Type A myelin sheet. This is the usual form of the sheet. When rolled up around an axon and sectioned in the indicated plane, it results in the usual type A configuration diagrammed in *A'*. *B*, Type B myelin sheet. The continuous surrounding cytoplasmic rim contains formed organelles. When rolled up around an axon and sectioned in the indicated plane, it results in the type B configuration diagrammed in *B'·C*, Type C myelin sheet. An extension of the lateral cytoplasmic rim intrudes into the myelin sheet. When rolled up around an axon and sectioned in the indicated plane, it results in a type C configuration including an isolated cytoplasmic island as diagrammed in *C'·D*, Type D myelin sheet. The irregularly widened inner rim is indented by a cleft of extracellular space. When rolled up around an axon and sectioned in the indicated plane, it results in a type D configuration including an apparently unconnected cell process as diagrammed in *D'·E*, Type E myelin sheet. The lateral rim is folded into the myelin sheet. When rolled up around an axon and sectioned in the indicated plane, it results in a type E configuration including two complete concentric myelin sheaths both spiraling in the same direction as indicated in *E'·F*, A myelin sheet derived from the unrolling of a myelin sheath in the peripheral nervous system. The outer cytoplasmic rim is much wider than in the central nervous system and consists of the entire cell body of the Schwann cell, including the nucleus (*N*). Furthermore, two thickened, vertical cytoplasmic ridges, roughly parallel to the lateral rims, are present (*S-L*) which give rise to the incisures of Schmidt-Lantermann when seen in longitudinal section. The outer rim is bordered by a basement membrane (*BM*). The inner and lateral rims, of course, are devoid of a basement membrane since, in the rolled up sheath, no basement membrane intervenes between the inner loop and the axon (*A*) or between adjacent lateral loops. When rolled up around an axon and sectioned in the indicated plane, it results in a typical peripheral myelin sheath as diagrammed in *F'*.

the inner loop, the outer loop, or both that participate with the lateral loops to account for the increase in the number of lamellae during development?

Let us consider the consequences if only the outer loop provided the myelin necessary to increase the number of lamellae with no participation by the inner loop. Under these circumstances, only one mechanism of sheath formation is apparent to us. It has often been stated that, in contrast to those in the peripheral nervous system, the outer loops in the central nervous system cannot rotate around the axon since they are connected to the glial cells which are effectively anchored due to their multiple processes (6, 25, 30, 37). Thus, if myelin formation does not occur at the inner loop, but is confined to the outer and lateral loops, the sheath must rotate around the axon as a rigid cylinder constantly thickening and elongating at each end.

If, however, myelin formation does indeed occur at the inner loop in addition to, or instead of, at the outer loop, the sheath would increase its number of turns by the motion of the inner loop as it deposits the newly formed myelin behind itself. A serious difficulty with this hypothesis, however, was raised by Lampert (18). He pointed out that after the first few turns the resulting tightening would prohibit the further advance of the inner loop.

To overcome this very cogent objection, we have resorted to the concept that adjacent myelin lamellae slip over each other. Conclusive evidence that myelin sheaths have the capacity to undergo such slippage was reported previously (9), although the concept of slippage was not made explicit at that time. In these reports, severe axonal swelling was observed with concomitant distention of the myelin sheath to many times its former diameter. However, the intra- and interlamellar distances within the sheath were indistinguishable from those of the nondistended sheaths. To us the only apparent explanation of this phenomenon is that adjacent myelin lamellae slipped past each other, much as a clock mainspring unwinds; this results in fewer turns and a much larger internal diameter. The results of studies of tin intoxication (1), in which tremendous focal intralamellar spaces appeared at the intraperiod line, might be explained similarly.

Therefore, we feel justified in offering the suggestion that myelin formation does occur at the inner loop as well as at the lateral loops. As a matter of fact, there is no compelling reason to believe that myelin formation occurs at the outer loop.

It should be pointed out that it is the inner and lateral loops that are in immediate contact with the axon. When one recognizes the fact that, for myelin formation to occur, there seems to be necessary a specific interaction between an axon and a myelin-forming cell (how else could one explain the fact that myelin forms exclusively around axons), then perhaps it is to be expected that myelin formation is limited to those parts of the myelin-forming cell which are in immediate contact with the axon itself.

The authors would like to acknowledge their gratitude to Dr. H. M. Zimmerman, Chief, Laboratory Division, Montefiore Hospital and Medical Center, for his constant encouragement, advice and support throughout this project. Furthermore, we are indebted to Dr. S. Levine, Professor of Pathology, New York Medical College, for his aid in performing many of the experimental procedures.

This investigation was supported by The Sandy Schneider Memorial Fund of the Montefiore Hospital and Medical Center.

Received for publication 1 February 1967.

REFERENCES

1. ALEU, F. P., R. KATZMAN, and R. D. TERRY. 1963. Fine structure and electrolyte analyses of cerebral edema induced by alkyl tin intoxication. *J. Neuropathol. Exptl. Neurol.* **22**:403.
2. ANDRES, K. H. 1965. Über die Feinstruktur besonderer Einrichtungen in markhaltigen Nervenfasern des Kleinhirns der Ratte. *Z. Zellforsch. Mikroskop. Anat.* **65**:701.
3. ARNOLD, H., and H. M. ZIMMERMAN. 1943. Experimental brain tumors. III. Tumors produced with dibenzanthracene. *Cancer Res.* **3**:682.
4. BARGMANN, W., and E. LINDNER. 1964. Über den Feinbau des Nebennierenmarkes des Igels (*Erinaceus europeus* L.). *Z. Zellforsch. Mikroskop. Anat.* **64**:868.
5. BUNGE, M. B., R. P. BUNGE, and G. D. PAPPAS. 1962. Electron microscopic demonstration of connections between glia and myelin sheaths in the developing mammalian nervous system. *J. Cell Biol.* **12**:448.
6. BUNGE, M. B., R. P. BUNGE, and H. RIS. 1961. Ultrastructural study of remyelination in an experimental lesion in adult cat spinal cord. *J. Biophys. Biochem. Cytol.* **10**:67.

7. BUNGE, R. P., and P. M. GLASS. 1965. Some observations on myelin-glial relationships and on the etiology of the cerebrospinal fluid exchange lesion. *Ann. N. Y. Acad. Sci.* **122**:15.
8. DALTON, A. J. 1955. A chrome-osmium fixative for electron microscopy. *Anat. Record.* **121**:652.
9. HIRANO, A., S. LEVINE, and H. M. ZIMMERMAN. 1967. Experimental cyanide encephalopathy: Electron microscopic observations of early lesions in white matter. *J. Neuropathol. Exptl. Neurol.* **26**:200.
10. HIRANO, A., H. M. ZIMMERMAN, and S. LEVINE. 1964. Fine structure of cerebral fluid accumulation. III. Extracellular spread of cryptococcal polysaccharide in the acute stage. *Am. J. Pathol.* **45**:1.
11. HIRANO, A., H. M. ZIMMERMAN, and S. LEVINE. 1966. Myelin in the central nervous system as observed in experimentally induced edema in the rat. *J. Cell Biol.* **30**:397.
12. IKUTA, F., and H. M. ZIMMFRMAN. 1965. Virus particles in reactive cells induced by intracerebral implantation of dibenzanthracene. *J. Neuropathol. Exptl. Neurol.* **24**:225.
13. KERR, F. W. L. 1966. The ultrastructure of the spinal tract of the trigeminal nerve and the substantia gelatinosa. *Exptl. Neurol.* **16**:359.
14. KLATZO, I., A. PIRAUX, and E. J. LASKOWSKI. 1958. The relationship between edema, blood brain barrier, and tissue elements in a local brain injury. *J. Neuropathol. Exptl. Neurol.* **17**:548.
15. KRUGER, L., and D. S. MAXWELL. 1966. Electron microscopy of oligodendrocytes in normal rat cerebrum. *Am. J. Anat.* **118**:411.
16. LAATSCH, R. H., and W. M. COWAN. 1966. A structural specialization at nodes of Ranvier in central nervous system. *Nature.* **210**:757.
17. LAMPERT, P. W. 1965. Electron microscopic studies on the vascular permeability and the mechanism of demyelination in experimental allergic encephalomyelitis. *J. Neuropathol. Exptl. Neurol.* **24**:11.
18. LAMPERT, P. W. 1965. Demyelination and remyelination in experimental allergic encephalomyelitis. *J. Neuropathol. Exptl. Neurol.* **24**:371.
19. LAMPERT, P. W. 1966. Electron microscopic observations on the mechanism of demyelination in experimental allergic encephalomyelitis. *In* Proceedings of the Fifth International Congress of Neuropathology. *Excerpta Med. Ser. No. 100.* 259.
20. LEE, J. C., and L. BAKAY. 1966. Ultrastructural changes in the edematous central nervous system. II. Cold-induced edema. *Arch. Neurol.* **14**:36.
21. LEVINE, S., A. HIRANO, and H. M. ZIMMERMAN. 1964. The reaction of the nervous system to cryptococcal infection: An experimental study with light and electron microscopy. *In* Infections of the Nervous System: Proceedings of the Association for Research in Nervous and Mental Disease. H. M. Zimmerman, editor. The Williams & Wilkins Co., Baltimore. In press.
22. LEVINE, S., and W. STYPULKOWSKI. 1959. Experimental cyanide encephalopathy. *Arch. Pathol.* **67**:306.
23. LEVINE, S., H. M. ZIMMERMAN, E. J. WENK, and N. K. GONATAS. 1963. Experimental leukoencephalopathies due to implantation of foreign substances. *Am. J. Pathol.* **42**:97.
24. LUFT, J. 1961. Improvements in epoxy resin embedding methods. *J. Biophys. Biochem. Cytol.* **9**:409.
25. MATURANA, H. R. 1960. The fine anatomy of the optic nerve of anurans—an electron microscope study. *J. Biophys. Biochem. Cytol.* **7**:107.
26. METUZALS, J. 1963. Ultrastructure of myelinated nerve fibers in the central nervous system of the frog. *J. Ultrastruct. Res.* **8**:30.
27. PALAY, S. L., S. M. MCGEE-RUSSELL, S. GORDON, JR., and M. A. GRILL. 1962. Fixation of neural tissues for electron microscopy by perfusion with solutions of osmium tetroxide. *J. Cell Biol.* **12**:385.
28. PETERS, A. 1960. The structure of myelin sheaths in the central nervous system of *Xenopus laevis* (Daudin). *J. Biophys. Biochem. Cytol.* **7**:121.
29. PETERS, A. 1960. The formation and structure of myelin sheaths in the central nervous system. *J. Biophys. Biochem. Cytol.* **8**:431.
30. PETERS, A. 1964. Further observations on the structure of myelin sheaths in the central nervous system. *J. Cell Biol.* **20**:281.
31. PETERS, A. 1964. Observations on the connexions between myelin sheaths and glial cells in the optic nerves of young rats. *J. Anat.* **98**:125.
32. PETERS, A. 1966. The node of Ranvier in the central nervous system. *Quart. J. Exptl. Physiol.* **51**:229.
33. ROBERTSON, J. D. 1959. Preliminary observations on the ultrastructure of nodes of Ranvier. *Z. Zellforsch. Mikroskop. Anat.* **50**:553.
34. ROSS, L. L., M. B. BORNSTEIN, and G. M. LEHRER. 1962. Electron microscopic observations of rat and mouse cerebellum in tissue culture. *J. Cell Biol.* **14**:19.
35. TORACK, R. M., R. D. TERRY, and H. M. ZIMMERMAN. 1959. The fine structure of cerebral fluid accumulation: I. Swelling secondary to cold injury. *Am. J. Pathol.* **35**:1135.
36. UZMAN, B. G. 1964. The spiral configuration of myelin lamellae. *J. Ultrastruct. Res.* **2**:208.
37. UZMAN, B. G., and G. M. VILLEGAS. 1960. A comparison of nodes of Ranvier in sciatic nerves with node-like structures in optic nerves of the mouse. *J. Biophys. Biochem. Cytol.* **7**:761.